Quantum Science and Technology

OPEN ACCESS

RECEIVED
10 September 2018

REVISED
30 November 2018

ACCEPTED FOR PUBLICATION
4 December 2018

PUBLISHED
22 January 2019

PAPER

Levitated electromechanics: all-electrical cooling of charged nano- and micro-particles

Daniel Goldwater[1,5], **Benjamin A Stickler**[2], **Lukas Martinetz**[2], **Tracy E Northup**[3], **Klaus Hornberger**[2] **and James Millen**[4,5]

[1] Department of Physics and Astronomy, University College London, Gower Street, London WC1E 6BT, United Kingdom
[2] University of Duisburg-Essen, Faculty of Physics, Lotharstraße 1, D-47048 Duisburg, Germany
[3] Institut für Experimentalphysik, Universität Innsbruck, Technikerstraße 25, A-6020 Innsbruck, Austria
[4] Department of Physics, King's College London, Strand, London, WC2R 2LS, United Kingdom
[5] Authors to whom any correspondence should be addressed.

E-mail: dan.goldwater@nottingham.ac.uk **and** james.millen@kcl.ac.uk

Keywords: optomechanics, electromechanics, levitated optomechanics, levitated electromechanics, hybrid system

Supplementary material for this article is available online

Abstract

We show how charged levitated nano- and micro-particles can be cooled by interfacing them with an *RLC* circuit. All-electrical levitation and cooling is applicable to a wide range of particle sizes and materials, and will enable state-of-the-art force sensing within an electrically networked system. Exploring the cooling limits in the presence of realistic noise we find that the quantum regime of particle motion can be reached in cryogenic environments both for passive resistive cooling and for an active feedback scheme, paving the way to levitated quantum electromechanics.

1. Introduction

The control of nano- and micro-scale objects in vacuum is of great importance for a wide range of applications [1], from the study of individual proteins [2], viruses [3] and bacteria [4], to the simulation of astrophysical processes via the study of dusty plasmas [5], to the detection of tiny forces [6, 7]. It is predicted that the motion of levitated nanoparticles can be controlled even at the quantum level [8–11], enabling studies of macroscopic quantum physics [12] and the contribution of levitated high quality-factor oscillators in quantum technologies as coherent storage or signal transduction devices.

To achieve quantum control of nano- and micro-particles, their motion must be cooled towards the quantum regime, which is viable via optical cavity cooling [8–11, 13–17] or parametric feedback [18, 19], achieving temperatures below 500 μK (a few tens of motional quanta). However, these optomechanical methods are limited by the very optical fields that are used for cooling, through optical absorption [20, 21], photon scattering [19], and instability at low pressures [6, 13, 20, 22].

Charged particles can instead be levitated in ion traps [23, 24], with trapped atomic ions at the forefront of quantum information processing technology [25, 26]. Their motion can be detected and cooled via their coupling to the trap electrodes [27, 28], either resistively or using active feedback methods [29, 30]. Extending these techniques to nano- and micro-particles will enable manipulation and control of massive charged particles by electronic circuitry. This opens the field of *levitated electromechanics*, holding the promise of scalability and network integration.

In this work, we present an all-electrical levitation, detection and cooling scheme for charged nano- and micro-particles, which will operate stably under vacuum conditions while avoiding optical scattering and absorption heating. Our simulations show that sub-Kelvin particle temperatures are achievable with room temperature circuitry via resistive and feedback cooling. The applicable range of sizes, from sub-nanometer to several micrometers, and materials, including metallic clusters, dielectric particles and biological objects, illustrates the universality of this technology. Under ambient conditions, levitated electromechanics will offer a

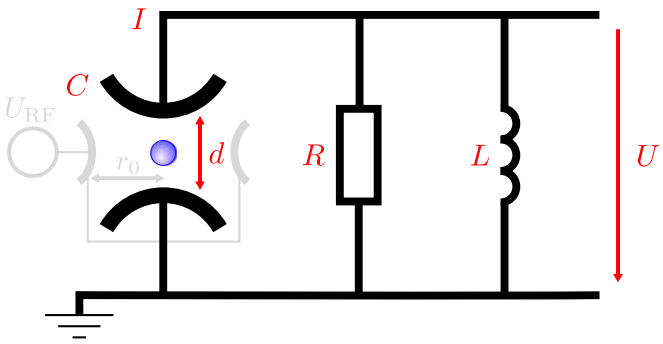

Figure 1. Circuit diagram for the electronic detection of charged particle motion for an object levitated in a quadrupole ion trap (gray diagram). The motion of the trapped particle is picked up by the endcap electrodes separated by d, and induces a current I in the circuit. A voltage U is generated across the resistance R of the circuit. Resonant detection is possible by forming either a series or parallel RLC circuit (with parallel illustrated here), where the capacitance C is due to the trap electrodes plus any parasitic capacitance.

simple and robust pre-cooling method for optical cavity cooling, and state-of-the-art force sensing. This scheme is suited to cryogenic environments, where millikelvin temperatures allow reaching the deep quantum regime.

We first derive the equations-of-motion of a charged particle coupled to an RLC circuit, and show how they can be quantized. Then we discuss the electronic detection of motion, followed by the potential to cool through passive-resistive and active feedback methods. Finally we discuss the application of levitated electromechanics to displacement and force sensing.

2. Equations of motion

We consider a spherical particle of mass M and charge q levitated in a potential $V(z)$, with trapping frequency ω_z, which is levitated between plates of separation d and capacitance C. As illustrated in figure 1 the two electrodes are joined via an inductance L to form an LC circuit. While in this work we envision that $V(z)$ is provided by a Paul trap, with the capacitor formed by the endcap electrodes, we note that the levitating potential could also be optical. The equations of motion for a charged particle in a Paul trap are provided in appendix A. The interaction with electrostatic mirror charges formed in the endcap electrodes is negligible for the trap parameters considered below.

The dynamics of the charged particle can be derived using the Shockley–Ramo theorem [31, 32]. It relates the current I flowing in the circuit with the particle momentum $p = M\dot{z}$ and the voltage drop U across the capacitor. For now we consider the conservative LC circuit neglecting resistance, yielding

$$I = -\frac{q}{d}\frac{p}{M} + C\dot{U}. \tag{1}$$

We use the circuit-charge Q on the capacitor as the generalized coordinate of the circuit, so that the magnetic flux through the inductor $\Phi = L\dot{Q}$ acts as its associated canonical momentum, and exploit Kirchhoff's law, $U = -\dot{\Phi}$, to obtain the canonical equations-of-motion

$$\dot{Q} = \frac{\Phi}{L}, \tag{2a}$$

$$\dot{\Phi} = -\frac{Q}{C} - \frac{q}{Cd}z. \tag{2b}$$

The first term in equation (2b) gives rise to a harmonic oscillation of frequency $\omega_{LC} = 1/\sqrt{LC}$, while the second term accounts for the linear coupling to the particle position z.

The back-action of the circuit dynamics onto the particle motion can be derived by noting that the voltage offset U across the capacitor induces a constant force $-qQ/Cd$ acting on the particle. Neglecting charging effects due to the formation of mirror charges, which are on the order of $q^2/MCd^2 \ll \omega_z^2$, one thus obtains the equations-of-motion for the particle:

$$\dot{z} = \frac{p}{M}, \tag{2c}$$

$$\dot{p} = -\partial_z V(z) - \frac{q}{Cd}Q. \tag{2d}$$

Equation (2d) describes the coupled classical dynamics of a charged particle trapped inside an LC circuit. The Hamiltonian function associated with these dynamics can be identified

$$H = \frac{\Phi^2}{2L} + \frac{Q^2}{2C} + \frac{p^2}{2M} + V(z) + \frac{q}{Cd}Qz. \tag{3}$$

For harmonic $V(z)$ the particle-circuit system behaves as two linearly coupled harmonic oscillators.

2.1. Dissipation

We now consider the role of a resistor, of resistance R and temperature T_R, connected in series with the LC circuit. Its action is described by adding the damping and diffusion term $-\Gamma\Phi + \sqrt{2\Gamma L k_B T_R}\,\xi(t)$ to equation (2b). Here, the damping rate of the circuit is $\Gamma = R/L$, and the second term with white noise $\xi(t)$, i.e. $\langle \xi(t+\tau)\xi(t)\rangle = \delta(\tau)$, describes circuit thermalization at temperature T. Due to the linear coupling between the circuit and the particle (equation (3)), the particle will thermalize with the circuit resistance at temperature T_R. The corresponding timescale $1/\gamma$ is determined by the circuit parameters R, L and C as well as by the particle charge q and mass M. Dissipation in a parallel RLC circuit can be described in a similar fashion by adding a friction and diffusion term, with parallel friction rate $\Gamma = 1/RC$, to the equation-of-motion for the circuit charge.

2.1.1. Adiabatic damping

If the circuit follows the particle motion adiabatically we can eliminate the former from the equations-of-motion in equation (2). Neglecting diffusion for the moment, one obtains from equations (2a) and (2b) the quasi-static expressions for a series RLC circuit

$$Q \simeq -\frac{q}{d}z + \frac{\Gamma LCq}{dM}p, \tag{4a}$$

$$\Phi \simeq -\frac{qL}{Md}p. \tag{4b}$$

These yield the non-conservative equations of motion for the particle

$$\dot{z} = \frac{p}{M}, \tag{5a}$$

$$\dot{p} = -\partial_z V(z) - \frac{\Gamma L q^2}{Md^2}p, \tag{5b}$$

which allows us to identify the adiabatic damping rate

$$\gamma_{\rm ad} = \frac{\Gamma L q^2}{Md^2}. \tag{6}$$

A similar calculation for the parallel RLC circuit yields $\gamma_{\rm ad} = 0$ since the capacitor is effectively shorted out in this scenario. In the derivation of equation (5) we neglected the additional attractive force related to the appearance of electrostatic mirror charges. This contribution is negligible in the present case, and causes a fractional frequency shift of $q^2/MCd^2\omega_z^2 \sim 10^{-6}$.

2.1.2. Damping on resonance

If the circuit is on resonance with the particle motion, $\omega_{LC} = \omega_z$, the oscillatory dynamics of the particle can effectively cancel the inductance, leading to a boosted friction rate. This can be made evident by Fourier-transforming the particle-circuit equations-of-motion for the series RLC circuit and eliminating the circuit

$$\omega^2\tilde{z}(\omega) = \left(\omega_z^2 + \frac{q^2\omega_z^2}{MCd^2}\frac{\omega^2-\omega_z^2}{(\omega^2-\omega_z^2)^2+\omega^2\Gamma^2}\right)\tilde{z}(\omega) + \mathrm{i}\frac{q^2\omega_z^2}{MCd^2}\frac{\omega\Gamma}{(\omega^2-\omega_z^2)^2+\omega^2\Gamma^2}\tilde{z}(\omega). \tag{7}$$

For $\Gamma^2 \gg |\omega^2 - \omega_z^2|$, this equation yields the on-resonance particle friction rate

$$\gamma_{\rm res} = \frac{q^2}{MC\Gamma d^2}, \tag{8}$$

which increases with decreasing circuit dissipation. A similar calculation for the parallel RLC circuit yields the same result for the friction rate. This resonant enhancement of friction is in agreement with the damping rate observed for trapped atomic ions and electrons [33, 34]. Note that the series adiabatic friction rate (6) is equal to the parallel on-resonance damping rate (8).

2.2. Quantum dynamics

We consider the situation where particle and circuit are cooled to their ground-state or close to it. The coupled quantum dynamics of the combined particle-series RLC circuit state ρ can be modeled by the Lindblad master equation [35]

$$\partial_t \rho = -\frac{\mathrm{i}}{\hbar}[\mathsf{H}, \rho] - \frac{\mathrm{i}\Gamma}{4\hbar}[\{\mathsf{Q}, \Phi\}, \rho] + \frac{\Gamma}{2}\left(\mathsf{L}\rho\mathsf{L}^\dagger - \frac{1}{2}\{\mathsf{L}^\dagger\mathsf{L}, \rho\}\right), \tag{9}$$

where H is the quantized Hamiltonian (operators are denoted by sans-serif characters), and the Lindblad operator is

$$\mathsf{L} = \frac{\sqrt{4Lk_\mathrm{B}T_R}}{\hbar}\mathsf{Q} + \frac{\mathrm{i}}{\sqrt{4Lk_\mathrm{B}T_R}}\Phi. \tag{10}$$

The completely positive master equation (9) describes the Markovian thermalization dynamics of the particle-circuit state ρ. For large circuit temperatures, where the term proportional to $1/T_R$ can be neglected, one obtains

$$\partial_t \rho = -\frac{\mathrm{i}}{\hbar}[\mathsf{H}, \rho] + \frac{\Gamma}{2\mathrm{i}\hbar}[\mathsf{Q}, \{\Phi, \rho\}] - \frac{\Gamma L k_\mathrm{B} T_R}{\hbar^2}[\mathsf{Q}, [\mathsf{Q}, \rho]]. \tag{11}$$

The second term on the right hand side describes damping of the circuit momentum Φ with friction rate Γ, while the third term describes charge diffusion. The corresponding diffusion constant $\Gamma L k_\mathrm{B} T_R$ is in accordance with the fluctuation-dissipation relation. If the trapping potential is harmonic the master equation describes thermalization towards the Gibbs equilibrium $\rho_\mathrm{eq} = \exp(-\mathsf{H}/k_\mathrm{B}T_R)/Z$, and the expectation values of the canonical phase-space observables exhibit classical thermalization dynamics (equation (2)).

3. Detection of the particle motion

Experiments demonstrating trapping of single electrons [36, 37], ions [38] and protons [30] as well as electron [27] and proton [39] clouds have noted that it is possible to detect the classical motion of the charged particle(s) via the image current I that they generate in the endcap electrodes of Paul or Penning traps [33]. We now show that this is also possible for spherical nano- and micro-scale particles. Under the assumption that $\Gamma \gg \omega_z$ the circuit adiabatically follows the particle motion, and equation (1) reduces in lowest order of the particle velocity to

$$I = -\frac{q\eta}{d}\dot{z}, \tag{12}$$

where we have introduced the geometrical factor η to account for the shape of the pick-up electrodes, which we assign the realistic value of $\eta = 0.8$ for slightly parabolically shaped electrodes [28]. The maximum velocity given by the equipartition theorem is $\dot{z}_\mathrm{max} = \sqrt{k_\mathrm{B}T_\mathrm{CM}/M}$, where T_CM is the center-of-mass temperature of the particle. This implies a peak induced current of

$$I_\mathrm{max} = \frac{q\eta}{d}\sqrt{\frac{k_\mathrm{B}T_\mathrm{CM}}{M}}. \tag{13}$$

The scaling $I_\mathrm{max} \propto q/\sqrt{M}$ is favorable when working with highly charged massive particles. A silica sphere of radius $r_\mathrm{S} = 1\ \mu$m ($M = 5.5 \times 10^{12}$ amu) and realistic charge $q = 10^6\, e$ (appendix B), where e is the elementary charge, will induce a comparable current to the atomic ion $^{88}\mathrm{Sr}^+$.

4. Resistive cooling

As demonstrated in section 2.1, connecting the endcap electrodes to an *RLC* circuit serves to dissipate the induced current and thus damp the particle motion. The ensuing friction rate (equation (8)) on resonance ($\omega_{LC} = \omega_z$) can be written as

$$\gamma_\mathrm{res} = \left(\frac{q\eta}{d}\right)^2 \frac{R_\mathrm{eff}}{M}, \tag{14}$$

where we introduced the effective resistance R_eff [28, 34]. For a series *RLC* circuit $R_\mathrm{eff} = Q_\mathrm{f}^2 R$, while for a parallel RLC circuit it reads $R_\mathrm{eff} = \omega_z L Q_\mathrm{f}$, with the circuit quality factor $Q_\mathrm{f} = \omega_z/\Gamma$.

Tuned circuits with $Q_\mathrm{f} = 25\,000$ have been used to cool N_2^+ ions [40], and it is proposed to exploit high Q_f quartz crystal oscillators connected in parallel with the endcaps to further boost resistive cooling [41]. For a modest $Q_\mathrm{f} = 100$ and $R = 100\ \mathrm{M}\Omega$, an $r_\mathrm{S} = 1\ \mu$m, $q = 10^6\, e$ silica sphere at room temperature would generate a signal of ~100 mV for electrodes separated by 1 mm.

Resistive cooling is illustrated in figure 2, where the motion of a charged microsphere in a quadrupole ion trap is numerically simulated including all sources of noise, as outlined in appendix A. From equation (14), it is clear that to increase the damping rate, one can increase R_eff or q, as verified in figure 2(a), where equation (14) is compared to the results of the numerical simulation, with the agreement illustrating that realistic experimental

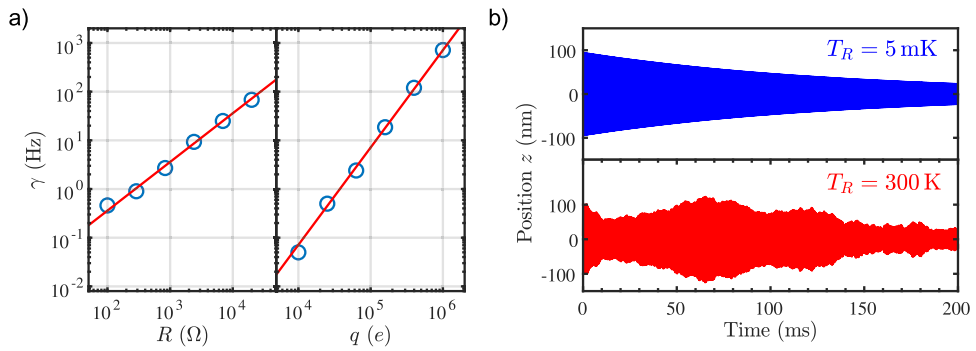

Figure 2. Resistive cooling: (a) variation in the momentum damping rate γ of a charged particle coupled to a circuit, with resistor value R and particle charge q (open circles: simulation equation (26), solid lines: equation (14)). (b) Simulated particle trajectories for two different circuit temperatures T_R, illustrating that the particle thermalizes with the circuit. The parameters in this figure unless stated otherwise are: $T_{\text{in}} = 1000$ K, $r_{\text{S}} = 1$ μm, $q = 10^5$ e, $d = 1$ mm, $Q_{\text{f}} = 100$, $R = 100$ MΩ, $T_R = 300$ K.

noise has little effect on the damping rate. The scaling of the damping rate $\gamma \propto q^2/M$ is favorable for highly-charged massive particles.

The dissipation of energy across R is accompanied by heating due to Johnson–Nyquist noise [28, 33, 34], modeled as a white voltage-noise source $\mathcal{V}_R$ of width $\sqrt{4k_{\text{B}}T_R R_{\text{eff}}}$, where T_R is the temperature of the circuit. For a description of how noise is added to the simulations of trapped particle motion, see appendix A. In the absence of other noise sources, the particle will equilibrate to the temperature of the circuit T_R, as indicated by the thermal trajectory in figure 2(b). Hence, to reach low temperatures via resistive cooling, cryogenic circuitry is required [34]. Note that it is possible to design ion trap geometries to resistively cool all three degrees-of-freedom, for example by using a ring electrode which is split into segments [28, 42].

Even under ambient conditions, resistive cooling can be useful to stabilize trapped particles, for example against collisions with residual gas molecules [6, 13, 20], or to pre-cool massive particles, which in general possess initial motional energies far above room temperature due to the loading mechanism [15, 43]. Furthermore, avoiding optical fields removes motional heating due to scattering of photons.

To consider the limits of resistive cooling, we consider operation in a state-of-the-art dilution refrigerator at 5 mK. By considering the quadrupole ion trap stability parameters, as defined by equation (23) in appendix A, an $r_{\text{S}} = 1$ μm silica sphere with $q = 10^6$ e can have stable frequencies of $\omega_z > 2\pi \times 1$ MHz, which would correspond to reaching a phonon occupancy of $n = k_{\text{B}}T_{\text{CM}}/(\hbar\omega_z) < 100$.

5. Feedback cooling

Since we can detect the motion of a charged particle via the endcap voltage U, we can feed this signal back onto the endcaps to dynamically control the particle's motion. Figure 3 shows a schematic of this process, where an amplifier with gain G generates the voltage GU on the lower endcap electrode. With the appropriate phase shift between U and GU, this either amplifies or cools the motion [29, 38, 44].

In the scenario depicted in figure 3, the charged particle sees a voltage U_{fb} which is generated by the voltage difference between the two endcap electrodes:

$$U_{\text{fb}} = (1 - G)U. \tag{15}$$

At $G = 1$ the circuit resistance that the particle sees $R_{\text{fb}} = (1 - G)R_{\text{eff}}$ and the thermal noise is tuned out. Explicitly, in this simple model the temperature T_{CM} of the particle is reduced to $T_{\text{CM}} = (1 - G)T_R$. Simultaneously, the feedback damping rate $\gamma_{\text{fb}} \propto R_{\text{fb}}$ goes to zero as G approaches unity, $\gamma_{\text{fb}} = (1 - G)\gamma$. Charged nano- and micro-particles are stable in Paul traps on the timescale of months [15], somewhat negating the necessity for rapid damping in the absence of other noise sources.

For a more realistic description, it is necessary to include the voltage noise added by the feedback amplifier $\mathcal{V}_{\text{fb}}$, as illustrated in figure 3. Noise added due to collisions with gas molecules and electrode surface potentials is considered in the supplementary information is available online at stacks.iop.org/QST/4/024003/mmedia, and included in the simulations of the particle motion presented in figures 2 and 4, and can be neglected. This noise voltage has an associated noise temperature T_{fb}^{n} defined through $\mathcal{V}_{\text{fb}} = \sqrt{4k_{\text{B}}T_{\text{fb}}^{\text{n}}R_{\text{amp}}B}$, where R_{amp} is the resistance of the feedback amplifier, and B is its bandwidth. This noise adds in quadrature with the uncorrelated voltage noise $\mathcal{V}_R$ [44], leading to a total

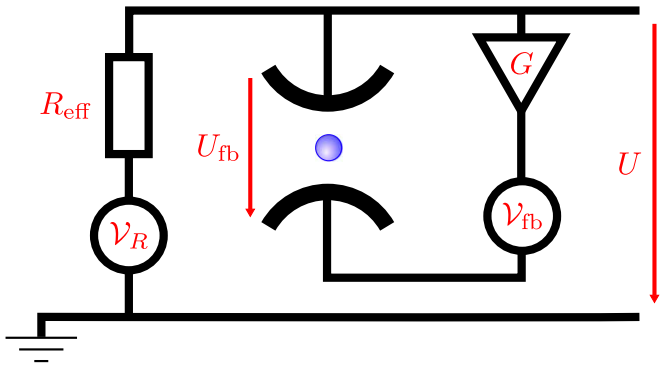

Figure 3. Circuit diagram for the feedback control of charged particle motion. The motion of the particle induces a voltage U across the effective resistance $R_{\rm eff}$. An amplifier of gain G feeds this voltage back onto one of the endcap electrodes, effectively shorting out the Johnson–Nyquist noise at $G = 1$. The feedback amplifier introduces voltage noise $\mathcal{V}_{\rm fb}$.

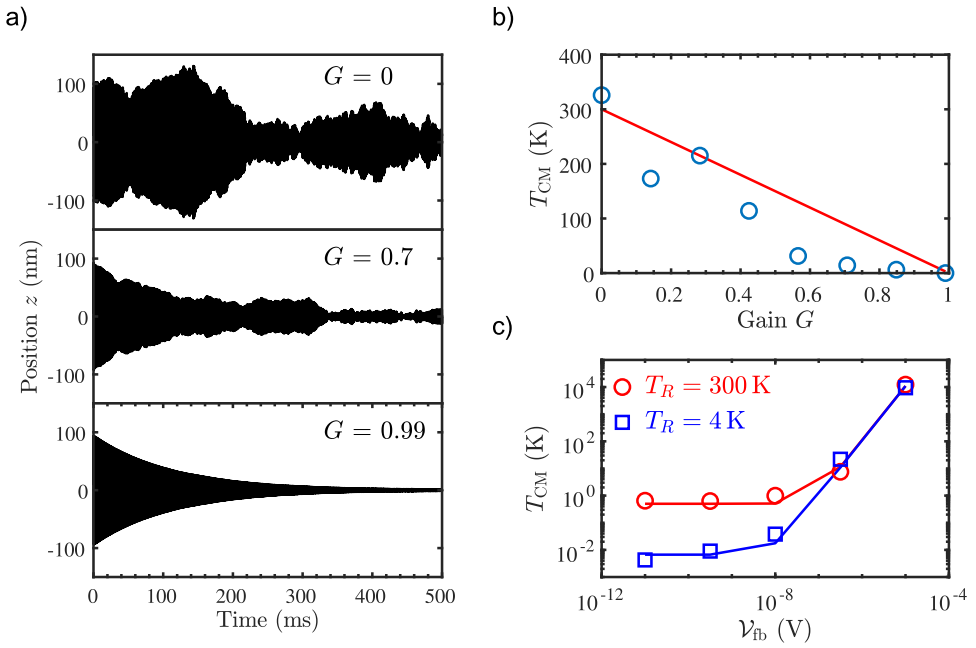

Figure 4. Feedback cooling: (a) simulated particle trajectories showing the effect of feedback gain G. Variation in simulated particle equilibrium temperature $T_{\rm CM}$ with (b) amplifier gain G (open circles: simulation equation (26), solid line: equation (17), disagreement due to the finite run-time of the simulations), and (c) feedback amplifier noise voltage $\mathcal{V}_{\rm fb}$ at two different circuit temperatures T_R, with $G = 0.95$ (open circles: simulation equation (26), solid line: equation (17)). The parameters in this figure unless stated otherwise are: $T_{\rm in} = 1000$ K, $r_{\rm S} = 1$ μm, $q = 10^5$ e, $d = 1$ mm, $Q_{\rm f} = 100$, $R = 100$ MΩ, $\mathcal{V}_{\rm fb} = 10^{-10}$ V, $T_R = 300$ K.

$$\mathcal{V}_{\rm total} = \sqrt{(1-G)^2\mathcal{V}_{\rm R}^2 + G^2\mathcal{V}_{\rm fb}^2}, \tag{16}$$

and a particle equilibrium temperature

$$T_{\rm CM} = (1-G)\,T_R + \frac{G^2}{1-G}T_{\rm fb}^{\rm n}. \tag{17}$$

A simulation of the effect of feedback on the particle dynamics is shown in figure 4(a). A comparison of equation (17) and simulation is shown both for a variation in feedback gain G and in noise voltage $\mathcal{V}_{\rm fb}$ in figures 4(b) and (c) respectively. Equation (17) is minimized at $G \approx 1 - \sqrt{T_{\rm fb}^{\rm n}/T_R}$, yielding a minimum temperature $T_{\rm fb}^{\rm min} \approx 2\sqrt{T_{\rm fb}^{\rm n}\,T_R}$. The noise voltage $\mathcal{V}_{\rm fb}$ of commercial amplifiers can be sub-nanovolt, yielding sub-kelvin particle temperatures even with room temperature circuitry, as illustrated in figure 4(c).

Using state-of-the-art cryogenic SQUID amplifiers with noise temperatures below 20 μK [45] with $T_R = 5$ mK, it would be possible to use feedback to reduce the temperature to below 100 μK. This corresponds to the motional ground-state for few-MHz oscillation frequencies. Hence, with cryogenic operation, this system is in-principle suitable for cooling micron-sized charged particles to the quantum ground-state.

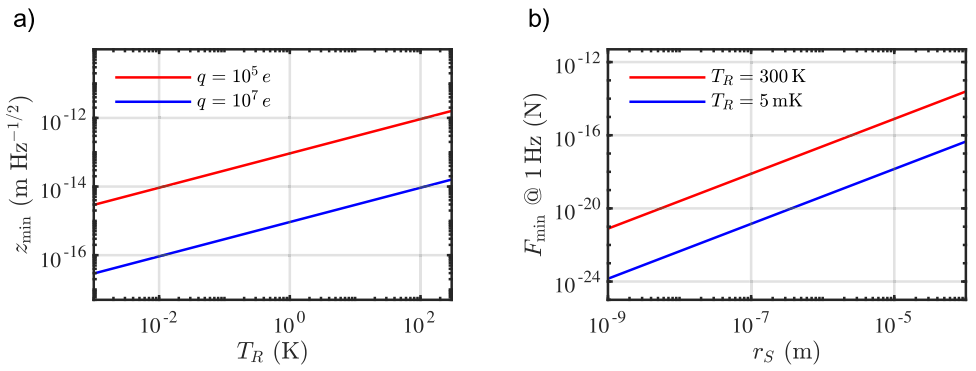

Figure 5. Sensing: (a) minimum detectable particle displacement with a 1 Hz measurement bandwidth as a function of the circuit temperature T_R, for two different values of particle charge q, with $\omega_z = 2\pi \times 1$ MHz. (b) Minimum detectable force with a 1 Hz measurement bandwidth, as a function of particle size r_S (silica sphere), for two different circuit temperatures T_R, assuming that the particle thermalizes with the circuit. The parameters in this figure unless stated otherwise are: $r_S = 1\ \mu$m, $d = 1$ mm, $Q_f = 100$, $R = 100$ MΩ.

6. Position, size and force sensitivity

Opto- and electro-mechanical devices make excellent sensors, due to their low mass and ability to couple to a wide range of forces [46], and they have found application in genetics, proteomics, microbiology and studies of DNA [47]. Their sensitivity is limited by dissipation to the environment, a problem which gets worse with decreasing physical size [48]. By levitating the oscillator, many dissipation processes are removed, which has enabled force sensing with optically levitated microparticles on the zepto-Newton scale [49].

The smallest displacement of a charged particle that can be measured through an induced voltage in this system is limited by noise. The dominant source is the Johnson–Nyquist noise voltage $\mathcal{V}_R = \sqrt{4k_B T_R R_{\rm eff} \Delta\nu}$, where $\Delta\nu$ is the detection bandwidth. Since one can make a phase sensitive detection [33], $\Delta\nu$ can be very small. By considering the point at which the induced signal U is equal to $\mathcal{V}_R$, it is straightforward to show that the minimum detectable particle velocity on resonance is

$$\dot{z}_{\rm min} = \sqrt{\frac{4k_B T_R \Delta\nu}{M\gamma}}, \tag{18}$$

since other sources of noise are negligible (supplementary information). For a harmonic oscillator one has $z_{\rm min} = \dot{z}_{\rm min}/\omega_z$. The variation in $z_{\rm min}$ with T_R and q is shown in figure 5(a). Considering a $r_S = 500$ nm silica sphere, $\gamma = 1$ kHz, and $\omega_z = 2\pi \times 1$ MHz, even at room temperature (300 K) this corresponds to 10^{-11} m Hz$^{-\frac{1}{2}}$ resolution, and at a cryogenic temperature of 5 mK, $< 10^{-15}$ m Hz$^{-\frac{1}{2}}$ resolution. The zero-point fluctuation of such a particle is $z_{\rm zpf} = \sqrt{\hbar/2M\omega_z} = 8 \times 10^{-15}$ m.

When considering the force sensitivity of a harmonic oscillator, the minimum detectable force is $F_{\rm min} = \sqrt{4k_B T_{\rm CM} M\gamma_{\rm CM}\Delta\nu}$, where $\gamma_{\rm CM}$ is the damping rate on its motion [49]. In our case, the dominant damping without feedback is resistive γ, as defined in equation (14). This cannot be made arbitrarily low, since small γ means we detect less signal U, which must in turn be greater than the noise voltage $\mathcal{V}_R$. Hence, we have the requirement

$$IR_{\rm eff} > \sqrt{4k_B T_R R_{\rm eff}\Delta\nu}. \tag{19}$$

Using equations (13) and (14), and assuming that the particle is in thermal equilibrium with the circuit $T_{\rm CM} = T_R$, we find the simple expression $\gamma > 4\Delta\nu$, which is the value of the resistive damping required to measure above the thermal noise in a given bandwidth. In other words, the measurement time must be on the order of the ring-down time ($1/\gamma$). This yields a force sensitivity

$$F_{\rm min} = \gamma\sqrt{k_B T_R M}. \tag{20}$$

The variation in $F_{\rm min}$ with particle size and temperature is shown in figure 5(b). Practically, choosing a low value of γ will lead to long thermalization times, requiring a stable experiment, although particles in ion traps are stable on month-timescales. Using equation (20), with a 1 Hz measurement bandwidth, for an $r_S = 100$ nm silica sphere, $F_{\rm min}$ at 300 K is 8×10^{-19} N, and at 5 mK is 3×10^{-21} N, comparable to state-of-the-art optical systems [49]. It is worth noting that it is possible to levitate lower-mass particles in an ion trap than optically, due to an increased trap depth, making the electromechanical system attractive for sensing applications.

Finally, using equations (13) and (19), it is possible to detect particles which satisfy the following relation

$$\frac{q}{\sqrt{M}} > \sqrt{\frac{2\Delta\nu}{R_{\rm eff}}}\frac{d}{\eta}. \tag{21}$$

As an example, this means that using realistic experimental parameters ($R = 100$ MΩ, $Q_{\rm f} = 100$, $\eta = 0.8$, $d = 1$ mm, $\Delta\nu = 1$ Hz), it would be possible to detect singly charged particles with masses up to 5×10^6 amu.

7. Discussion

We have demonstrated that *levitated electromechanics*, where charged particles levitated in an ion trap are interfaced with an *RLC* circuit, can be used for electronic detection, cooling and precision sensing. Using feedback, sub-kelvin temperatures are achievable with room temperature circuitry, and we predict that working in a cryogenic environment will enable ground-state cooling for micron-sized particles.

Levitated electromechanics is compatible with optomechanical systems. A hybrid levitated opto-/electro-mechanical set-up is suitable for cooling deep into the quantum regime, and for the production of interesting mechanical quantum states, such as squeezed states [50]. Charged particles equilibrate with the trapping circuitry, which acts as a highly controllable thermal bath, making the system suitable for studies of low-dissipation thermodynamics [51].

Acknowledgments

JM is grateful for discussions with Andrew Geraci, and for funding from EPSRC project EP/S004777/1. DG would like to thank Peter Barker for useful discussions, and is supported by the Controlled Quantum Dynamics Centre for Doctoral Training at Imperial College London. BS and LM acknowledge support by Deutsche Forschungsgemeinschaft (DFG—411042854). TN acknowledges support from Austrian Science Fund (FWF) Projects Y951-N36 and F4019-N23.

Appendix A. Equations of motion in a quadrupole ion trap

For the purposes of this work, we consider only motion along the z-axis between the endcap electrodes of a spherical quadrupole ion trap. The equation-of-motion when driven by a voltage $U_{\rm AC}(t) = U_{\rm DC} + U_0\cos(\omega_D t)$ is

$$M\ddot{z} - \frac{M\omega_D^2}{4}[a_z - 2q_z\cos(\omega_D t)]z = 0, \tag{22}$$

where ω_D is the drive frequency, and a_z, q_z are stability parameters

$$\begin{aligned} a_z &= \frac{4U_{\rm DC}\eta q}{M\omega_D^2 r_0^2} \\ q_z &= -\frac{2U_0\eta q}{M\omega_D^2 r_0^2}, \end{aligned} \tag{23}$$

with $\eta = 0.8$ is a geometric factor, M the mass of the particle, and $2r_0$ the separation between the RF electrodes (or the diameter of the ring electrode). In what follows, we set $U_{\rm DC} = 0$ (and hence $a_z = 0$). This yields a secular frequency in the z-direction of $\omega_z = \omega_D q_z/2\sqrt{2}$.

Feedback, as discussed in section 5, acts as a force proportional to the velocity $\dot{z}$, since it depends on the induced current I (see equation (12)). Hence, with feedback, the equation-of-motion reads:

$$M\ddot{z} + M\gamma_{\rm fb}\dot{z} + \frac{M\omega_D^2}{2}q_z\cos(\omega_D t)z = 0. \tag{24}$$

A.1. Inclusion of noise

We consider the influence of several noise sources: gas collisions at temperature $T_{\rm gas}$ through the damping rate $\gamma_{\rm gas}$ (see supplementary information); the Johnson–Nyquist noise of the circuit at the temperature T_R through the rate γ; and the noise of the feedback amplifier $\mathcal{V}_{\rm fb}$ with associated noise temperature $T_{\rm fb}^{\rm n}$ and damping rate $\gamma_{\rm fb}$.

We include each of these in our model via the fluctuation-dissipation theorem

$$\begin{aligned}\langle F_{\rm gas}(t+\tau)F_{\rm gas}(t)\rangle &= 2k_{\rm B}T_{\rm gas}\gamma_{\rm gas}M\delta(\tau)\\ \langle F_R(t+\tau)F_R(t)\rangle &= 2k_{\rm B}T_R\gamma M\delta(\tau)\\ \langle F^{\rm n}_{\rm fb}(t+\tau)F^{\rm n}_{\rm fb}(t)\rangle &= 2k_{\rm B}T^{\rm n}_{\rm fb}\gamma_{\rm fb}M\delta(\tau),\end{aligned} \tag{25}$$

for the gas, resistive, and feedback random force respectively.

The electrode surface noise, which is discussed in detail in the supplementary information, is included by considering the fluctuating force $\langle F_E(t+\tau)F_E(t)\rangle = q^2S_E(\omega_z)\delta(t-\tau)$, constructed noting that an electric field E generates a force qE on a particle of charge q [52].

Hence, the full equation-of-motion for the z-direction reads:

$$M\ddot{z} + M(\gamma_{\rm gas}+\gamma_{\rm res}+\gamma_{\rm fb})\dot{z} + \frac{M\omega_D^2}{2}q_z\cos(\omega_D t)z = F_{\rm gas}+F_{\rm res}+F_{\rm n,fb}+F_E. \tag{26}$$

Appendix B. Charging the particles

The resistive and feedback damping rates depend on the charge q of the trapped particle. A dielectric particle of radius $r_{\rm S}$ can hold a maximal negative charge [53] of about

$$\frac{q_{\rm neg}}{e} = -1 - 0.7\left(\frac{r_{\rm S}}{\rm nm}\right)^2, \tag{27}$$

and a maximal positive charge of [53]

$$\frac{q_{\rm pos}}{e} = 1 + 21\left(\frac{r_{\rm S}}{\rm nm}\right)^2. \tag{28}$$

This implies that a $r_{\rm S} = 1$ μm particle can hold up to 2×10^7 positive charges. Practically, 5 μm diameter melamine particles have been charged via positive ion bombardment (5 keV He ions) to hold $\sim 7\times10^6$ $|e|$ [54], significantly below the theoretical limit in equation (28).

Charging can be achieved via electron or ion bombardment [54–56], corona discharge [57] and adhesion of charged droplets. Not much is known about the charging limits for sub-micron particles, but it has been noted that, for smaller particles, secondary emission of charge from the bulk material can limit the maximum surface potential [56, 58]. Smaller spheres require higher electric fields to charge, as determined by the Pauthenier equation [57], which says that in a uniform electric field E, the maximum charge held by a sphere is

$$q_{\rm max} = 4\pi\epsilon_0 r_{\rm S}^2 pE, \tag{29}$$

where $p = 3$ for a conductor, and $p = 3\epsilon_{\rm r}/(\epsilon_{\rm r}+2)$ for a dielectric. Low charges on nano- [59] and micro-particles [55] are stable over timescales of hours.

ORCID iDs

Benjamin A Stickler https://orcid.org/0000-0001-9075-1008
Tracy E Northup https://orcid.org/0000-0002-1071-2218
Klaus Hornberger https://orcid.org/0000-0002-3145-1117
James Millen https://orcid.org/0000-0002-6950-3461

References

[1] Maher S, Jjunju F P M and Taylor S 2015 Colloquium: 100 years of mass spectrometry: perspectives and future trends *Rev. Mod. Phys.* **87** 113
[2] Bruce J E, Cheng X, Bakhtiar R, Wu Q, Hofstadler S A, Anderson G A and Smith R D 1994 Trapping, detection, and mass measurement of individual ions in a fourier transform ion cyclotron resonance mass spectrometer *J. Am. Chem. Soc.* **116** 7839–47
[3] Fuerstenau S D, Benner W H, Thomas J J, Brugidou C, Bothner B and Siuzdak G 2001 Mass spectrometry of an intact virus *Angew. Chem. Int. Ed.* **113** 559–62
[4] Peng W P, Yang Y C, Kang M W, Lee Y T and Chang H C 2004 Measuring masses of single bacterial whole cells with a quadrupole ion trap *J. Am. Chem. Soc.* **126** 11766–7
[5] Morfill G E and Ivlev A V 2009 Complex plasmas: an interdisciplinary research field *Rev. Mod. Phys.* **81** 1353–404
[6] Ranjit G, Atherton D P, Stutz J H, Cunningham M and Geraci A A 2015 Attonewton force detection using microspheres in a dual-beam optical trap in high vacuum *Phys. Rev.* A **91** 051805
[7] Kuhn S, Stickler B A, Kosloff A, Patolsky F, Hornberger K, Arndt M and Millen J 2017 Optically driven ultra-stable nanomechanical rotor *Nat. Commun.* **8** 1670
[8] Chang D E *et al* 2010 Cavity opto-mechanics using an optically levitated nanosphere *Proc. Natl Acad. Sci. USA* **107** 1005

[9] Barker P F and Schneider M N 2010 Cavity cooling of an optically trapped nanoparticle *Phys. Rev.* A **81** 023826
[10] Romero-Isart O, Juan M, Quidant R and Cirac J 2010 Toward quantum superposition of living organisms *New J. Phys.* **12** 033015
[11] Stickler B A *et al* 2016 Ro-translational cavity cooling of dielectric rods and disks *Phys. Rev.* A **94** 033818
[12] Arndt M and Hornberger K 2014 Insight review: testing the limits of quantum mechanical superpositions *Nat. Phys.* **10** 271–7
[13] Kiesel N *et al* 2013 Cavity cooling of an optically levitated submicron particle *Proc. Natl Acad. Sci. USA* **110** 14180–5
[14] Asenbaum P, Kuhn S, Nimmrichter S, Sezer U and Arndt M 2013 Cavity cooling of free silicon nanoparticles in high-vacuum *Nat. Commun.* **4** 2743
[15] Millen J, Fonseca P Z G, Mavrogordatos T, Monteiro T S and Barker P F 2015 Cavity cooling a single charged levitated nanosphere *Phys. Rev. Lett.* **114** 123602
[16] Kuhn S *et al* 2016 Nanoparticle detection in an open-access silicon microcavity *Appl. Phys. Lett.* **111** 253107
[17] Fonseca P Z G, Aranas E B, Millen J, Monteiro T S and Barker P F 2016 Nonlinear dynamics and strong cavity cooling of levitated nanoparticles *Phys. Rev. Lett.* **117** 173602
[18] Gieseler J, Deutsch B, Quidant R and Novotny L 2012 Subkelvin parametric feedback cooling of a laser-trapped nanoparticle *Phys. Rev. Lett.* **109** 103603
[19] Jain V, Gieseler J, Moritz C, Dellago C, Quidant R and Novotny L 2016 Direct measurement of photon recoil from a levitated nanoparticle *Phys. Rev. Lett.* **116** 243601
[20] Millen J, Deesuwan T, Barker P F and Anders J 2014 Nanoscale temperature measurements using non-equilibrium Brownian dynamics of a levitated nanosphere *Nat. Nano* **9** 425–9
[21] Hebestreit E, Reimann R, Frimmer M and Novotny L 2018 Measuring the internal temperature of a levitated nanoparticle in high vacuum *Phys. Rev.* A **97** 043803
[22] Vovrosh J, Rashid M, Hempston D, Bateman J, Paternostro M and Ulbricht H 2017 Parametric feedback cooling of levitated optomechanics in a parabolic mirror trap *J. Opt. Soc. Am.* B **34** 1421–8
[23] Paul W and Steinwedel H 1953 Ein neues massenspektrometer ohne magnetfeld *Z. Naturforsch.* A **8** 448–50
[24] Paul W 1990 Electromagnetic traps for charged and neutral particles *Rev. Mod. Phys.* **62** 531
[25] Duan L-M and Monroe C 2010 Colloquium: quantum networks with trapped ions *Rev. Mod. Phys.* **82** 1209
[26] Singer K *et al* 2010 Colloquium: trapped ions as quantum bits: essential numerical tools *Rev. Mod. Phys.* **82** 2609
[27] Wineland D and Dehmelt H G 1975 Principles of the stored ion calorimeter *J. Appl. Phys.* **46** 919
[28] Itano W M, Bergquist J C, Bollinger J J and Wineland D J 1995 Cooling methods in ion traps *Phys. Scr.* **1995** 106
[29] D'Urso B, Odom B and Gabrielse G 2003 Feedback cooling of a one-electron oscillator *Phys. Rev. Lett.* **90** 043001
[30] Guise N, DiSciacca J and Gabrielse G 2010 Self-excitation and feedback cooling of an isolated proton *Phys. Rev. Lett.* **104** 143001
[31] Shockley W 1938 Currents to conductors induced by a moving point charge *J. Appl. Phys.* **10** 635–6
[32] Sirkis M D and Holonyak N Jr 1966 Currents induced by moving charges *Am. J. Phys.* **34** 943–6
[33] Brown L S and Gabrielse G 1986 Geonium theory: physics of a single electron or ion in a Penning trap *Rev. Mod. Phys.* **58** 233
[34] Di Domizio S, Krasnick D, Lagomarsino V, Testera G, Vaccaronea R and Zavatarellia S 2015 Toward sub-Kelvin resistive cooling and non destructive detection of trapped non-neutral electron plasma *J. Instrum.* **10** P01009
[35] Breuer H-P and Petruccione F 2002 *The Theory of Open Quantum Systems* (Oxford: Oxford University Press)
[36] Wineland D, Ekstrom P and Dehmelt H 1973 Monoelectron oscillator *Phys. Rev. Lett.* **31** 1279
[37] D'Urso B, Van Handel R, Odom B, Hanneke D and Gabrielse G 2005 Single-particle self-excited oscillator *Phys. Rev. Lett.* **94** 113002
[38] Dehmelt H, Nagourney W and Sandberg J 1986 Self-excited mono-ion oscillator *Proc. Natl Acad. Sci. USA* **83** 5761–3
[39] Church D A and Dehmelt H G 1969 Radiative cooling of an electrodynamically contained proton gas *J. Appl. Phys.* **40** 3421–4
[40] Cornell E A *et al* 1989 Single-ion cyclotron resonance measurement of $M(CO^+)/M(N_2^+)$ *Phys. Rev. Lett.* **63** 1674
[41] Kaltenbacher T, Caspers F, Doser M, Kellerbauer A and Pribyl W 2011 Resistive cooling circuits for charged particle traps using crystal resonators *Rev. Sci. Instrum.* **82** 114702
[42] Horvath G Zs K, Thompson R C and Knight P L 1997 Fundamental physics with trapped ions *Contemp. Phys.* **38** 25–48
[43] Millen J, Kuhn S, Patolsky F, Kosloff A and Arndt M 2016 Cooling and manipulation of nanoparticles in high vacuum *Proc. SPIE* **9922** 99220C
[44] D'Urso B 2003 Cooling and self-excitation of a one-electron oscillator *PhD Thesis* Harvard University
[45] Vinante A, Mezzena R, Prodi G A and Vitale S 2001 Dc superconducting quantum interference device amplifier for gravitational wave detectors with a true noise temperature of 16 μK *Appl. Phys. Lett.* **79** 2597
[46] Metcalfe M 2014 Applications of cavity optomechanics *Appl. Phys. Rev.* **1** 031105
[47] Calleja M, Kosaka P M, San Paulo A and Tamayo J 2012 Challenges for nanomechanical sensors in biological detection *Nanoscale* **4** 4925
[48] Ekinci K L and Roukes M L 2015 Nanoelectromechanical systems *Rev. Sci. Instrum.* **76** 061101
[49] Ranjit G, Cunningham M, Casey K and Geraci A A 2016 Zeptonewton force sensing with nanospheres in an optical lattice *Phys. Rev.* A **93** 053801
[50] Genoni M G, Zhang J, Millen J, Barker P F and Serafini A 2015 Quantum cooling and squeezing of a levitating nanosphere via time-continuous measurements *New J. Phys.* **17** 073019
[51] Millen J and Gieseler J 2018 Levitated nanoparticles for microscopic thermodynamics: A review *Entropy* **20** 326
[52] Brownnutt M, Kumph M, Rabl P and Blatt R 2015 Ion-trap measurements of electric-field noise near surfaces *Rev. Mod. Phys.* **87** 1419
[53] Draine B T and Sutin B 1987 Collisional charging of interstellar grains *Astrophys. J.* **320** 803
[54] Velyhan A, Žilavý P, Pavlů J, Šafránková J and Němeček Z 2004 Ion beam effects on dust grains *Vacuum* **76** 447
[55] Schlemmer S, Illemann J, Wallert S and Gerlich D 2001 Nondestructive high-resolution and absolute mass determination of single charged particles in a three-dimensional quadrupole trap *J. Appl. Phys.* **90** 5410–8
[56] Kopnin S I, Morozova T I and Popel S I 2017 Electron beam action and high charging of dust particles *IEEE Trans. Plasma Sci.* **99** 1–3
[57] Adamiak K 2002 Rate of charging of spherical particles by monopolar ions in electric fields *IEEE Trans. Ind. Appl.* **38** 1001–8
[58] Cermák I, Grün E and Švestka J 1995 New results in studies of electric charging of dust particles *Adv. Space Res.* **15** 59–64
[59] Frimmer M, Luszcz K, Ferreiro S, Jain V, Hebestreit E and Novotny L 2017 Controlling the net charge on a nanoparticle optically levitated in vacuum *Phys. Rev.* A **95** 061801